

Pressure flow dynamics in cellular automata based nephron network model

Siva Manohar Reddy Kesu^{1*}, Hariharan Ramasangu²

¹ Faculty of Engineering and Technology, M S Ramaiah University of Applied Sciences, Bengaluru, India

² Research Division, Relecura. Inc, Bengaluru, India

ABSTRACT


Developing a whole kidney model is important for effective diagnostic procedures and treating kidney diseases. The modeling of a multi-nephron network aids in developing the whole kidney model. The key aspect of any nephron model is understanding the pressure dynamics. The governing equations for pressure dynamics in the kidney depend on the number of nephrons and their interactions. There are mathematical models to analyze the local and global behaviors of single and coupled nephrons. It is difficult to formulate governing equations for a whole kidney model. This necessitates the development of simulation models. Even the simulation models have only been developed for 72 nephrons. The complexity is involved in incorporating both local and global behaviors of nephrons. In this paper, a cellular automata (CA) framework has been proposed to study the global behavior of nephrons. The advantage of the proposed CA framework is its scalability and its ability to capture global dynamics without formulating the corresponding governing equations. The limitation of the CA framework is its inability to compare point-to-point local behavior. But the clinical findings suggest that global behavior gives significant information about the kidney. We have developed CA rules for 8-nephron, 16-nephron, 72-nephron and 100-nephron network models considering both rigid and compliance tubules. The CA rules with various initialization schemes produce different evolutionary patterns similar to the emergent dynamical behavior of nephrons obtained from experimental and numerical findings. Evolutionary patterns of the CA framework are related to normotensive and hypertensive pressure dynamics. The in-phase and out-of-phase synchronizations have also been observed in the CA evolutionary patterns. The irregular rhythm of the cardiovascular system may give rise to shock waves in the pressure dynamics of the kidney. This behavior has also been observed in the proposed CA framework.

Keywords: Nephron-network, Cellular automata, Hypertension, Emergent properties.

OPEN ACCESS

Received: May 9, 2022
Revised: November 30, 2022
Accepted: March 11, 2023

Corresponding Author:
Siva Manohar Reddy Kesu
smreddyyyy@cvsr.ac.in

 **Copyright:** The Author(s).
This is an open access article distributed under the terms of the [Creative Commons Attribution License \(CC BY 4.0\)](https://creativecommons.org/licenses/by/4.0/), which permits unrestricted distribution provided the original author and source are cited.

Publisher:
[Chaoyang University of Technology](https://www.cvsr.ac.in/)
ISSN: 1727-2394 (Print)
ISSN: 1727-7841 (Online)

1. INTRODUCTION

The kidney has a hierarchical physical composition, with the nephrons and arteries as pyramids. Nephrons are grouped and interact with the neighborhoods (Marsh et al., 2007). The functional structure of the kidney is closely related to its physical structure based on the arrangement of the nephron tubule with the tubuloglomerular feedback (TGF) mechanism and exhibits a similar hierarchy functional behavior. Hierarchy is a property of many complex systems (Ravasz and Barabási, 2003). Therefore, it would be desirable to capture this hierarchy explicitly in our model to existing nephron models, which only capture hierarchy implicitly (Thomas, 2016).

The expansion of nephron network models produces valid behavior in individual and multi-nephron systems. This hierarchical model has investigated the properties of coupling and interaction between nephrons. The dynamical behavioral examination into the study of multi-nephron systems focused on the whole kidney and its classified

properties rather than the properties of the single nephron. As part of this examination, the dynamical behavior of a complex 72-nephron system has been analyzed the system significantly to the larger than existing multi-nephron models (Moss et al., 2009; Thomas, 2016; Kanzaki et al., 2020; Khouhak et al., 2020; Layton, 2021).

Larger multi-nephron models have been developed as extensions of single and paired nephron models. Marsh et al. (2007) simulated 22 nephrons attached to a single distributing artery, demonstrating that nephrons with a sufficiently different loop of Henle lengths will not synchronize under realistic vascular coupling conditions. Marsh et al. (2013) simulated 16 nephrons connected via a branching structure of arteries, considering TGF in the nephrons, vascular coupling between nephrons, and myogenic response in the arteries. Moss et al. (2009) have simulated 72 nephrons using a network model that avoids the use of coupled differential equations. The model by Moss et al. has included only six lumped parameter nephrons but uses a significantly more detailed glomerulus and medulla structure to reproduce water and sodium urine formation from the rat over a range of experimental conditions (Laugesen, 2011; Moss and Thomas, 2014; Thomas, 2016; Khouhak et al., 2019; Marsh et al., 2019).

In particular, many kidneys physiological models are based on coupled non-linear differential equations, which require small time step sizes and become increasingly difficult to solve as the system of differential equations becomes more prominent in models containing more components. Network models, where the model consists of components that communicate at each time step, do not have this limitation on their size. Moss et al. (2009) and Marsh et al. (2013) have presented network-based kidney physiology models. Moss et al. (2009) showed theoretical scaling, indicating that the network modeling approach can simulate kidneys with 72 nephrons, as found in a human, but did not carry out such large-scale simulations.

Network nephron models have been developed using various analogies such as graph automata and resistance-current sources. The proposed paper develops the nephron network model considering up to 100 nephrons using the CA framework. The developed model uses the CA rules of the single nephron and coupled nephrons to get the original characteristics of the model (Kesu and Ramasangu, 2021a; b; 2022).

Mathematical models have also been developed using CA (Tokihito et al., 1996; Matsuya and Murata, 2013). The construction of the CA model from the discrete model is a systematic procedure with the help of ultradiscretization (UD) (Tokihito et al., 1996; Kesu and Ramasangu, 2021a).

The ultradiscretization procedure preserves the characteristics of the original governing equations (Murata, 2013). This made the revolution in the mathematical models get more interest in converting UD equations. The UD equations involve max-plus algebra, min-plus algebra, and mini-max algebra (Tokihito et al., 1996; Isojima et al., 2006; Ohmori and Yamazaki, 2015).

CA framework is a discrete dynamical system. The basic unit of the CA is the cell. A cell, $C(k, n)$ is a discrete block in a spatio-temporal region where “k” and “n” refer to kth discrete block in space and nth discrete block in time respectively. Both spatial and temporal dimensions are discretized. Each cell has two possible values, either 0 as white or 1 as black. The cell value at the next time instant, $C(k, n + 1)$, depends on $C(k - 1, n)$, $C(k, n)$ and $C(k + 1, n)$.

In the elementary cellular automata (ECA), there are 256 rules of evolution ranging from rule number 0 to rule number 255. The patterns of evolution of ECA exhibit a wide range of dynamical system behavior. The CA patterns are known to characterize dynamical systems of varied nature. Wolfram has divided the emergent behavior of ECA into four classes of dynamical systems. The fixed and homogeneous state is categorized under class I. The pattern consists of separated periodic regions grouped under class II. The Class III group shows a chaotic and aperiodic pattern. The class IV group shows complex and localized structures (Wolfram and Mallinckrodt, 1995; Wolfram, 2002).

The rule of evolution for CA rule 178 is $C(k, n + 1) = C(k - 1, n)C(k, n) + C(k, n)C(k + 1, n) + C(k + 1, n)C(k - 1, n)$. In CA rule number 206, $C(k, n + 1) = C(k - 1, n)C(k + 1, n) + C(k, n)$ is the rule of evolution. The rule of evolution for CA rule 226 is $C(k, n + 1) = C(k - 1, n)C(k, n) + C(k + 1, n)C(k, n)$. The rule of evolution for CA rule 238 is $C(k, n + 1) = C(k, n) + C(k + 1, n)$.

CAs are used in modeling biological systems such as the spread of disease (Matsuya and Murata, 2015). The advantages of the CA framework are the study of dynamical systems through their emergent properties, and simplicity in the rules of evolution. This is the aspect that has been used while modeling a dynamical system using the CA framework. In this work, the CA framework has been applied to study the emergent properties of pressure dynamics in multi-nephron network models.

The pressure perturbations from the cardiovascular system change the pressure in the kidney. The autoregulatory mechanism controls the pressure oscillations and keeps them in stable mode. The change in the autoregulatory mechanism leads to normotensive to hypertensive behavior. These global properties have been explicitly captured in the CA multi-nephron network model.

The pressure flow analysis in the single nephron model and interacting analysis in coupled nephron model has limited to capturing the complete behavior analysis of the kidney model. In this paper, we have modeled multi-nephrons interacting with each other, which produces various types of pressure oscillations with the TGF mediation. CA rules have been developed with the necessary assumptions for the nephron network model. The solutions from the CA model have been analyzed and compared with the experimental findings to understand pathological and physiological behavior. This dynamical

analysis gives a clear understanding of pressure oscillations while interacting with many nephrons and their autoregulatory mechanism. Multi-scale modeling of the multi-nephron model is a novel attempt using CA framework that captures the global emergent behavior of the multi-nephron interaction system.

2. MULTI-NEPHRON MODEL USING SINGLE NEPHRON AND COUPLED NEPHRON MODEL GOVERNING EQUATIONS

This modeling approach has considered the governing equations for glomerulus and nephron tubule. The governing equations of nephron tubule are formed using fluid pressure; flow rate; tubular radius, and solute concentration as dependent variables (Keener and Sneyd, 1998; Beard and Mescam, 2012; Layton and Edwards, 2014; Moss and Layton, 2014; Moss and Thomas, 2014; Ryu, 2014).

The governing equation, Equation 1, is the advective diffusion equation which describes tubular fluid flow pressure $P(x,t)$, nephron tubular radius $R(x, t)$, and flow rate of the fluid $Q(x,t)$. The nephron inflow pressure and the outflow pressure are considered boundary conditions (Layton and Edwards, 2014). The partial differential equations of the nephron tubule model are

$$\frac{\partial P(x,t)}{\partial t} = \frac{R^3(x,t)}{16\mu} \frac{dR}{dP} \frac{\partial^2 P(x,t)}{\partial x^2} + \frac{R^2(x,t)}{4\mu} \frac{dR}{dP} \frac{\partial R(x,t)}{\partial x} \frac{\partial P(x,t)}{\partial x} \quad (1)$$

$$\frac{\partial}{\partial t} (\pi R^2(x, t) C(x, t) - \frac{\partial}{\partial x} Q(x, t) C(x, t) - 2\pi R_{ss}(x) (\frac{V_{max}(x)C(x,t)}{K_M + C(x,t)} + \kappa(C(x, t) - C_e(x)))) \quad (2)$$

Equation 2, represents solute concentration in TAL. In proximal tubule (PT), 60% to 75% of water is reabsorbed into the interstitium, and Distal Tubule (DT) diffuses the water into the interstitium. In this paper we have assumed glomerulus, PT and DT as pre-ascending limb (Ryu, 2014). TAL is the major part in the active and passive transport mechanism. It is used to regulate the pressure and solute concentration. The time independent interstitial solute concentration is represented as $C_e(x)$. The active transport mechanism is incorporated through maximum active transport rate $V_{max}(x)$ (Michaelis-Menten-like kinetics) and Michaelis constant K_M . The transepithelial solute diffusion is denoted by back leak permeability κ . The solute transport mechanism in TAL is independent of $R(x, t)$ and is directly proportional to the steady state TAL radius $R_{ss}(x)$. The boundary condition $C(0, t)$ means that the fluid entering into the TAL has a constant solute concentration (Layton and Edwards, 2014).

$$R(x, t) = \alpha(P(x, t) - P_e) + \beta(x) \quad (3)$$

Interstitial pressure is represented as P_e , degree of tubular compliance of the nephron tubule is represented as α , and unpressurized TAL radius is represented as $\beta(x)$ along with the TAL.

$$P_0(t) = P_0(1 + K_1 \tanh(K_2((C_{op} - C(L, t - \tau)))) \quad (4)$$

Equations 3 and 4 represent the autoregulatory mechanism such as myogenic and TGF mechanism for the single nephron tubular model respectively. The initial condition when $t = 0$ is denoted by $C(L, t - \tau) = C_{op}$. Half range of pressure variation $P_0(t)$ is taken as K_1 and TGF sensitivity as K_2 . steady state TAL solute concentration at MD is C_{op} . solute concentration along MD is $C(L, t - \tau)$, where TGF delay is τ (Ryu, 2014).

The governing equations for the coupled nephron model are outlined. The flow pressure equation of the one nephron has been influenced by the other nephron, whereas the solute concentration equation within the nephron tubule is not affecting the other nephron.

$$\frac{\partial P(x,t)}{\partial t} = \frac{R^3(x,t)}{16\mu} \frac{dR}{dP} \frac{\partial^2 P(x,t)}{\partial x^2} + \frac{R^2(x,t)}{4\mu} \frac{dR}{dP} \frac{\partial R(x,t)}{\partial x} \frac{\partial P(x,t)}{\partial x} - \frac{\Phi(x,t)}{2\pi R} \frac{dR}{dP} \quad (5)$$

$$\alpha = \frac{dR}{dP}$$

$$\frac{\partial P(x,t)}{\partial t} = \frac{R^3(x,t)}{16\mu\alpha} \frac{\partial^2 P(x,t)}{\partial x^2} + \frac{R^2(x,t)}{4\mu\alpha} \frac{\partial R(x,t)}{\partial x} \frac{\partial P(x,t)}{\partial x} - \frac{\Phi(x,t)}{2\pi R\alpha} \quad (6)$$

$$P_0(t) = P_0 + K_1 \tanh(K_2(C_{op} - C_1(2L, t - \tau))) + \sum \phi K_1 \tanh(K_2(C_{op} - C_2(2L, t - \tau))) \quad (7)$$

The ϕ is the coupling effect in the Equation 7 gives the interaction between the two nephrons, which shows the in-phase and antiphase oscillations. The Equation 7 provides the autoregulatory mechanism of the nephron influenced by the other nephron.

3. CELLULAR AUTOMATA FRAMEWORK FOR MULTI NEPHRON NETWORK MODEL

The proposed nephron network model is shown in Fig. 1. Single nephron and coupled nephron have been modeled using CA. Nephron network models have been developed based on analyzing the CA rules developed from single and coupled nephron models. The CA rules for n-nephron have been arrived at based on Boolean, algebraic, neighborhood, and mathematical algorithms. The details for single nephron to n-nephron kidney models have been outlined.

The governing equations for the single nephron have been ultra-discretized using Cole-Hopf transformations and tropical discretization. CA rules for nephron tubules have been developed based on assumptions for the pressure and solute concentration parameters. The CA rules have been

developed for the pressure equation, considering the nephron tubule as rigid and compliance. The CA model parameter values N and M are lower and upper thresholds.

The single nephron tubular model as rigid tubular model considering radius of the tubule $R_1(x, t) = 0$ and parameters $N \ll M$. The ultradiscretized equation, Equation 8, is obtained from Equation 1 (refer Kesu and Ramasangu (2021b) for the detailed derivation).

$$P_1(x, t + 1) = P_1(x - 1, t) + \max[0, P_1(x, t) - M, P_1(x + 1, t) - N] - \max[0, P_1(x - 1, t) - M, P_1(x, t) - N] \quad (8)$$

CA Rule 178 has been obtained for the ultradiscretized Equation 8 for single nephron rigid tubular model refer Kesu and Ramasangu (2021a).

The single nephron tubular model as compliance tubular model considering radius the tubule $R_1(x, t) = P_1(x, t)$ and parameters $N \ll M$. The ultradiscretized equation, Equation 9, is obtained from Equation 1 (refer Kesu and Ramasangu (2022) for the detailed derivation).

The CA rule 206 has been obtained for the single nephron compliance tubular model ultradiscretized pressure Equation 9 refer Kesu and Ramasangu (2022).

$$P_1(x, t + 1) = P_1(x - 1, t) + 2P_1(x, t) + \max[2P_1(x, t), 4P_1(x, t) - M, 2P_1(x + 1, t) - N] - 2P_1(x - 1, t) - \max[2P_1(x - 1, t), 4P_1(x - 1, t) - M, 2P_1(x, t) - N] \quad (9)$$

The consider coupled nephron tubular model as compliance tubular model when resitivity of the tubule $R_1(x, t) = 0$ and parameters $N \gg M$, $B_3 + G - L_1 \approx N$, $B_2 \approx M$ and B_1 is very small value. The ultradiscretized equation, Equation 10, is obtained from Equation 6 (refer (Kesu and Ramasangu, 2021a) for the detailed derivation).

$$P_1(x, t + 1) = [P_1(x - 1, t) + B_1 + \max[P_1(x, t) - M, P_1(x + 1, t) + \max[B_2 - N, B_3 + G - L_1 - N]]] - \max[P_1(x - 1, t) - M, P_1(x, t) + \max[B_2 - N, B_3 + G - L_1 - N]] \quad (10)$$

The CA rule 226 has been obtained for the coupled nephron rigid tubular model ultradiscretized pressure Equation 10 refer Kesu and Ramasangu (2021b).

The coupled nephron tubular model as compliance tubular model considering radius of the tubule $R_1(x, t) = P_1(x, t)$ and parameters $N \gg M$, $B_3 + G - L_1 \approx N$, $B_2 \approx M$ and B_1 is very small value. The ultradiscretized equation, Equation 11, is obtained from Equation 6 (refer Kesu and Ramasangu (2021) for the detailed derivation).

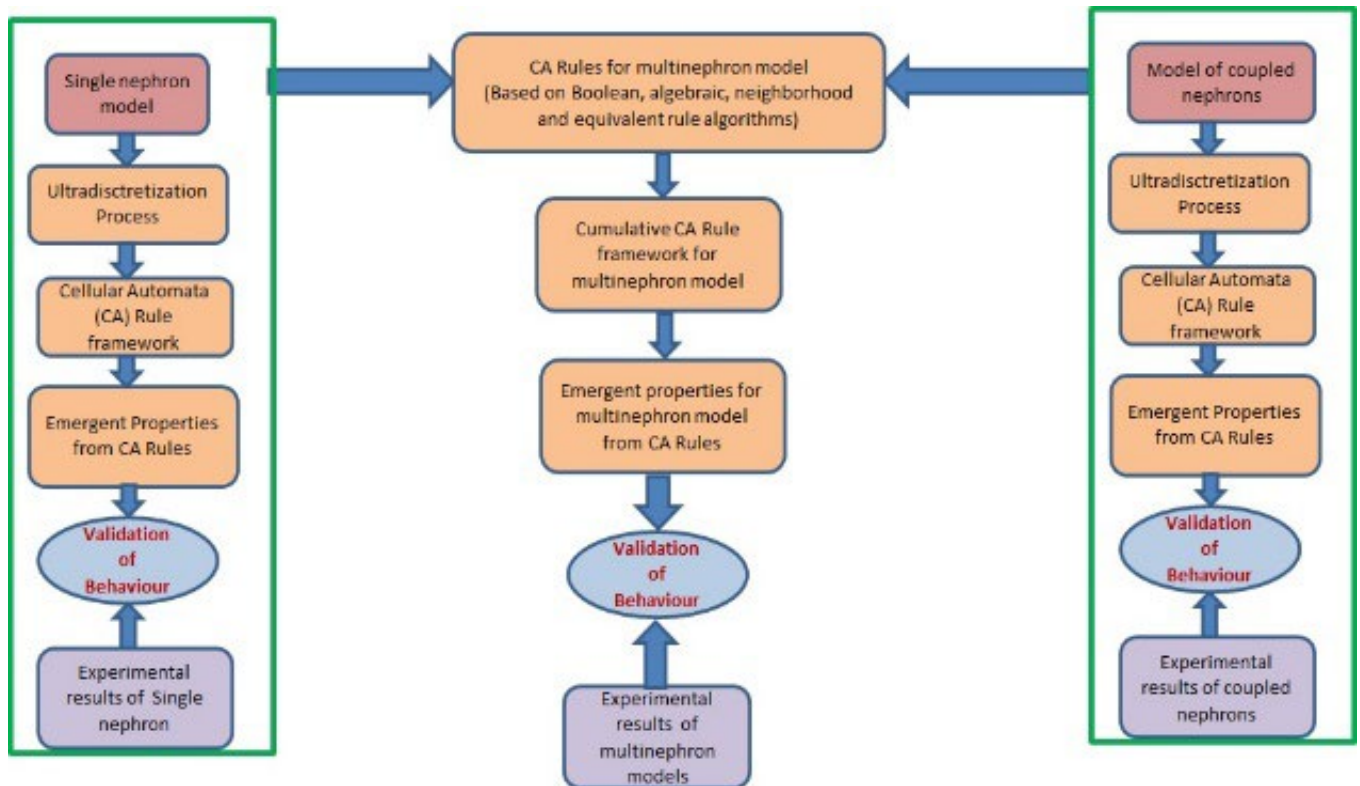


Fig. 1. Multi-nephron network model algorithm

$$P_1(x, t + 1) = [P_1(x - 1, t) + B_1 + 3R(x, t) + \max[0 + P_1(x, t) - M, P_1(x + 1, t) + \max[B_2 - N + R_1(x + 1, t) - R_1(x, t), B_3 + G - L_1 - N]] - \max[0 + P_1(x - 1, t) - M, P_1(x, t) + \max[B_2 - N + R_1(x, t) - R_1(x - 1, t), B_3 + G - L_1 - N]]] \quad (11)$$

The CA rule 238 has been obtained for the coupled nephron compliance tubular model ultradiscretized pressure Equation 11 refer Kesu and Ramasangu (2021b)

The CA rules obtained from the single nephron model and coupled nephron model have been analyzed. The arrival of the CA rule of coupled nephron model from the single nephron model has been analyzed based on the Boolean algebraic, neighborhood, and equivalent rules. The proposed cumulative algorithm using additive CA by Voorhees (1996) and modular arithmetic by Voorhees (2012) has been developed for getting the CA rules for the n-nephron model based on the various parameters shown in Fig. 1. The incremental CA rule obtained for the rigid tubular nephron network model is 48 based on the cumulative algorithm. In the compliance tubular model, The incremental CA rule obtained for the nephron network model is 32.

Table 1 shows the CA rules for an n-nephron network model obtained from the developed algorithm. The CA rules for up to 100 nephrons have been calculated. Table 1 shows the CA rules and the number of nephrons for a kidney model. The patterns have been analyzed in the next sections.

Table 1. CA rules for multi-nephron model

Sl no	Nephron number	Rigid model	Compliance model
1	8	4	175
2	10	100	239
3	16	133	176
4	72	16	183
5	100	56	85

4. RESULT AND DISCUSSION ON PRESSURE IN NEPHRON NETWORK MODEL FROM CELLULAR AUTOMATA MODEL

This section has been described the various nephron network models for the rigid and compliance tubule using CA. The behavior of pressure dynamics from the graphs has been compared with the behavior of pressure dynamics from evolutionary patterns obtained from CA rules as depicted in Table 2. The experimental data is not available as the clinical experiments have not been conducted. There is no access to the experimental data from previous experimental findings. Hence, the only way to validate the proposed CA framework is to compare the obtained results with that of the graphs published by the researchers who did the clinical experiments.

It has been compared with similar models of Moss (2009) and Thomas (2016). The results have been analyzed based on the Wolfram CA properties. The results from nephron network models of 8, 16 and 72 nephrons are presented and are compared with similar models of nephrons.

In the CA, the evolution takes place in a spatiotemporal grid. The origin cell is the left topmost cell. The spatial increment along the length of the tubule is along the X-axis (towards the right), and the temporal increment is along the Y-axis (towards the down). The dynamic state of cells is represented by white (0) and black (1), where black represents the cell value above the threshold and white represents the cell value below the threshold. The parameters in the ultradiscretized equations have to be considered for extreme case low and high for the analysis. The black represents for the cell value related to high and the white represents the cell value low. During the evolution of pressure dynamics, the threshold is necessary to differentiate from low value to high value. This threshold is more symbolic than the actual pressure dynamics threshold. Hence the specific threshold value is not required for CA evolution.

Table 2. CA behavior analysis of multi-nephron network model for rigid and compliance tubules in comparison with experimental findings

Sl No	Observed behavior in CA evolution	Equivalent dynamical behavior (Flake, 2000; Wolfram, 2018)	Wolfram class (Wolfram, 2002; Wolfram, 2018)	Observed experimental behavior from experimental findings (Moss, 2009; Niels-Henrik Holstein-Rathlou, 2011; Thomas, 2016)
1	Few pulses are propagating, and few are vanishing behavior	Simple, separated, and periodic in time and space and limit cycle oscillations	II	Period doubling (Out-of-phase synchronization)
2	Pulses have vanished	Fixed and limit point	I	Regular (In-phase synchronization)
3	Few pulses are propagating irregularly, and few pulses are sustained	Pseudo-random, aperiodic, and chaotic manner. Irregular	III	Irregular oscillations (Out-of-phase synchronization)
4	Pulses are propagating irregularly	Pseudo-random, aperiodic and chaotic manner. Irregular	III	Irregular oscillations (Out-of-phase synchronization)

Initialization in CA means assigning black cells in the first two rows. The initialization means there is a pressure perturbation as black in the initial section of the tubule for the TGF-inhibited case. The pressure perturbation has been initialized with black cells in the first layer, and perturbation as black has been initiated in the second layer below the previous section for the TGF-activated case. The evolved patterns have been analyzed and are shown to exhibit the emergent global properties of the physiological behavior of the nephron tubule. The evolutionary patterns from the CA rules have been categorized and compared with the Wolfram CA class framework.

Autoregulatory conditions for $P(x, t + 1)$ in the evolution of the CA rule as physiological properties of TGF in multi-nephron with in-phase synchronization are depicted in Table 3. The next stage goes low if the feedback signal is high for all eight possibilities, irrespective of input perturbation. If the feedback signal is low for all eight possibilities, the next state follows the CA rule for input perturbation.

Table 3. CA rule with TGF and in-phase synchronization

$P(x, t-1)$	$P(x-1, t)$	$P(x, t)$	$P(x+1, t)$	$P(x, t+1)$
1 (0)	0	0	0	0 (1 st bit of CA rule)
1 (0)	0	0	1	0 (2 nd bit of CA rule)
1 (0)	0	1	0	0 (3 rd bit of CA rule)
1 (0)	0	1	1	0 (4 th bit of CA rule)
1 (0)	1	0	0	0 (5 th bit of CA rule)
1 (0)	1	0	1	0 (6 th bit of CA rule)
1 (0)	1	1	0	0 (7 th bit of CA rule)
1 (0)	1	1	1	0 (8 th bit of CA rule)

Autoregulatory conditions for $P(x, t + 1)$ in the evolution of the CA rule as physiological properties of TGF with out-of-phase synchronization in multi-nephron are depicted in Table 4. The next stage goes low if the feedback signal is low for all eight possibilities, irrespective of input perturbation. If the feedback signal is high for all eight possibilities, the next state follows the CA rule for input perturbation.

Table 4. CA rule with TGF and out-of-phase synchronization

$P(x, t-1)$	$P(x-1, t)$	$P(x, t)$	$P(x+1, t)$	$P(x, t+1)$
1 (0)	0	0	0	1 st bit of CA rule (0)
1 (0)	0	0	1	2 nd bit of CA rule (0)
1 (0)	0	1	0	3 rd bit of CA rule (0)
1 (0)	0	1	1	4 th bit of CA rule (0)
1 (0)	1	0	0	5 th bit of CA rule (0)
1 (0)	1	0	1	6 th bit of CA rule (0)
1 (0)	1	1	0	7 th bit of CA rule (0)
1 (0)	1	1	1	8 th bit of CA rule (0)

The pulses vanish after initializing the black cell in the evolutionary pattern called pulse annihilation. It comes under Wolfram class I dynamical behavior of emergent properties. This type of behavior is observed when all the

nephrons are in-phase synchronization. The sustained and irregular pulse propagations in the evolutionary patterns have been categorized as Wolfram class II and III groups respectively. These behaviors have been observed when the nephrons in the multi-nephron network model are in out-of-phase synchronizations equivalent to irregular oscillations from the experimental findings. The CA rules have been derived when nephrons are considered rigid tubule (no change in tubular radius w.r.t pressure) and compliance tubule (change in tubular radius w.r.t pressure).

4.1. Nephron Network Model for N = 8 Nephrons

Fig. 2 (a) shows the pressure variations in a rigid nephron network model with the random initial state. This evolutionary pattern depicts the Pulse annihilation behavior. The evaluation shown from Fig. 2 (a) comes under the group of class I in Wolfram dynamical class behavior. The initialized pulses have been annihilated in the time evolution. This leads to regular normal pulse propagation. The eight nephron model with in-phase oscillations produces normal stable conditions in the functioning of the kidney.

Fig. 2 (b) shows the pressure variations in a rigid nephron network model with random initial states. The pulse produced on the left side has been propagated at the same space over the next iteration. This type of evolutionary pattern comes under class II group of Wolfram CA rules. The pulses will be continuously developed when nephrons are not synchronized.

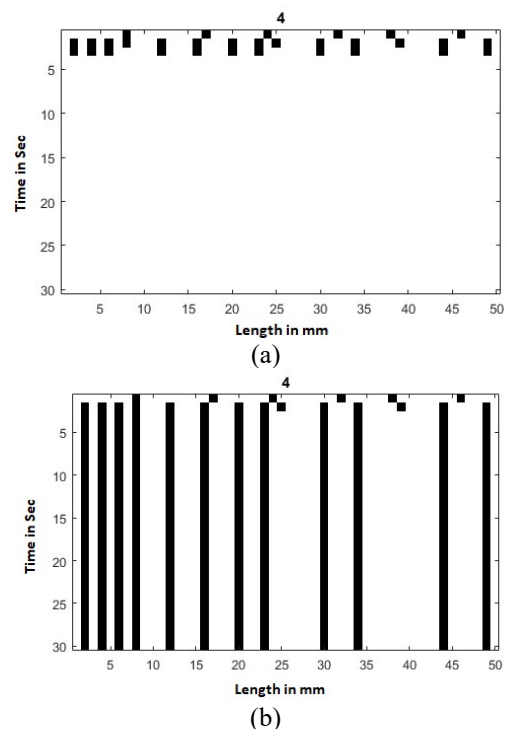


Fig. 2. Pressure variations in rigid nephron network model for CA rule 4 (a) with in-phase random initial states. (b) with out-of-phase random initial states for CA rule 4

Fig. 3 (a) shows the pressure variations in the compliance nephron network model with random initial states. The random initialization of the pulses develops the irregular pulse propagation in further iterations based on observation from the pattern evolution. This evolution pattern comes under class III from the Wolfram ECA rules group. The pulse propagated in the eight nephrons compliance model produces period-doubling oscillations. The pulses are moved from period doubling to chaotic oscillations when we trigger the pulses as perturbations at the time of initialization.

Fig. 3 (b) shows the pressure variations in the compliance nephron network model with random initial states. It exhibits the irregular pulse generation at the time evolution observed from the pattern. It comes under the class III group of Wolfram ECA rules. The observations have been made from the figure as the pulses show the shock wave oscillations. However, the pulse initialized at the starting space length is stable in further time iteration. The 8-nephron compliance multi-nephron network model depicts the clinical property as anti-phase oscillation among the nephrons produces chaotic oscillations.

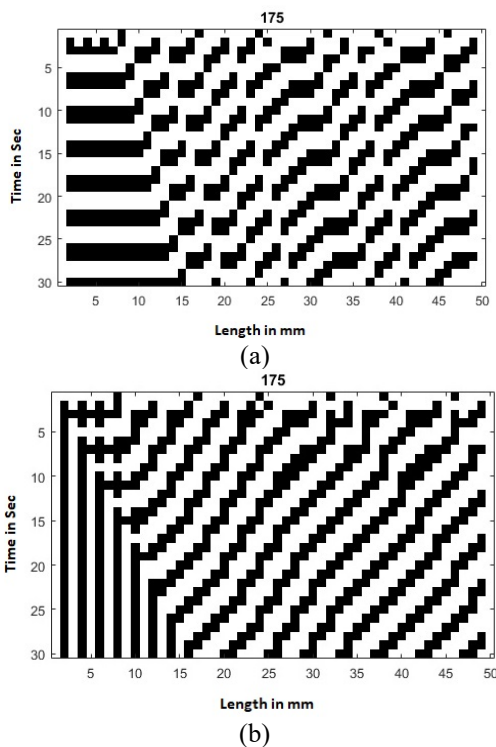


Fig. 3. Pressure variations in compliance nephron network model for CA rule 175 (a) with in-phase random initial states. (b) with out-of-phase random initial states

4.2. Nephron Network Model for N = 10 Nephrons

Fig. 4 (a) shows the pressure variations in a rigid nephron network model with the random initial state exhibits the pulse annihilation property. The evaluatory pattern comes under class I group of Wolfram CA properties. The

ten nephron model illustrates the behavior as in-phase oscillations produces normal stable conditions in the functioning of the kidney even in this random initialization. The perturbations have been settled down in a very short period of time and 10-nephron network model is in healthy condition.

Fig. 4 (b) shows the pressure variations in the rigid nephron network model with random initial states in the first row and second row. The observation made from the figure shows that the mixed propagation of the pulses which comes under class II group. The pulse is high and constant in some discrete space, and other discrete space produces suppressed oscillations. The ten nephrons rigid model with out-of-phase oscillations produces regular oscillations.

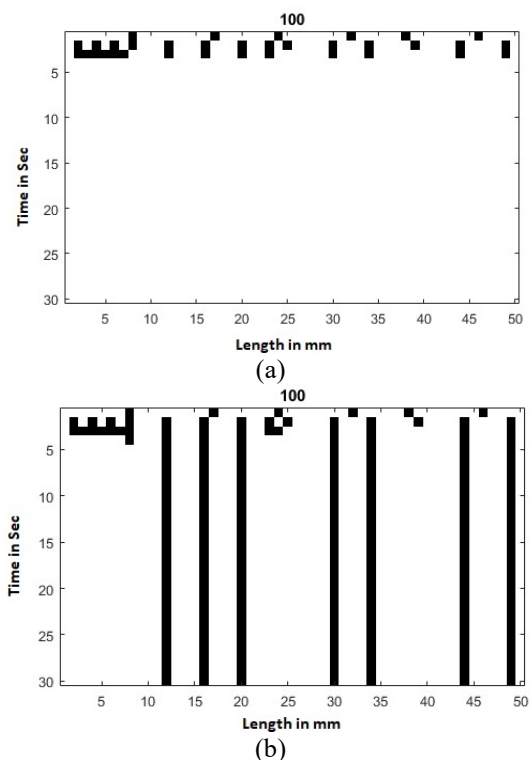


Fig. 4. Pressure variations in rigid nephron network model for CA rule 100 (a) with in-phase random initial states. (b) with out-of-phase random initial states

Fig. 5 (a) shows the pressure variations in compliance nephron network model with random initial states. The regular pulse propagation has been observed in the initial space length. The random initialization of the pulses produces irregular oscillations in the compliance ten nephron model for further iterations. These irregular and unstable oscillations have become normal over a period of time. This pattern has been observed in the class III group of Wolfram CA rules.

Fig. 5 (b) shows the pressure variations in the compliance nephron network model with random initial states. It exhibits irregular pulse generation at the time of evolution. It shows chaotic pulse propagation when there are random

perturbations have been applied. This type of irregular pulse can be settled to normally high-pressure pulses and causes hypertensive pressure variations. The ten nephrons compliance tubule model with anti-phase oscillations produces asynchronous pulse propagations.

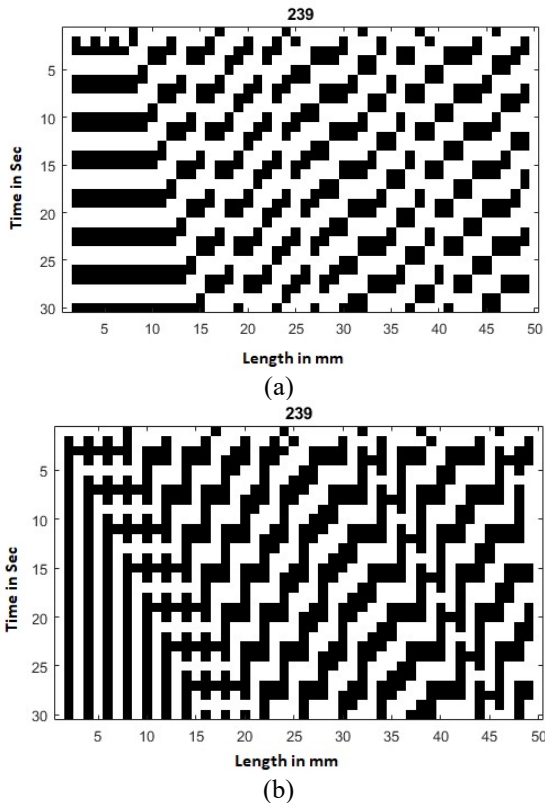


Fig. 5. Pressure variations in compliance nephron network model for CA rule 239 (a) with in-phase random initial states. (b) with out-of-phase random initial states

4.3. Nephron Network Model for N = 16 Nephrons

Fig. 6 (a) shows the pressure variations in a rigid nephron network model with the random initial state. The pulse produced initially is constant at the same space over the evolution of the rule. The perturbation applied to the 16 nephron network model shows the pulses are high at the same space over time. The evaluation comes from Fig. 6 (a) shows class II Wolfram properties. Even in this random initialization, the 16 nephron network model with in-phase oscillations produces normal stable conditions slightly above the threshold in the functioning of the kidney.

Fig. 6 (b) shows the pressure variations in the rigid nephron network model with random initial states in the first and second rows. The observation made from the figure shows the mixed propagation of the pulses. The pulse is high and constant in some discrete space, and other discrete space produces suppressed oscillations. The 16 nephrons rigid model with out-of-phase oscillations produces irregular oscillations.

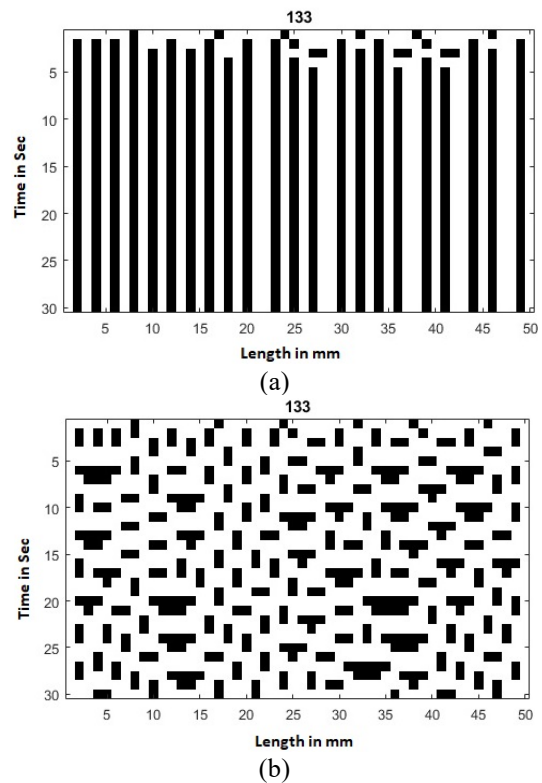


Fig. 6. Pressure variations in rigid nephron network model for CA rule 133 (a) with in-phase random initial states. (b) with out-of-phase random initial states

Fig. 7 (a) shows the pressure variations in the compliance nephron network model with random initial states. Regular pulse propagation has been observed in the initial space length. The random initialization of the pulses produces regular oscillations in the compliance 16 nephron network model for further iterations. These regular and stable oscillations have become normal over a period of time. This pattern has been observed in the class II group of Wolfram CA rules. The distortion produced from the perturbations has been settled and shifted towards the right.

Fig. 7 (b) shows the pressure variations in the compliance nephron network model with random initial states. It exhibits regular pulse generation at the time of evolution. It shows that stable pulse propagation, even though there are random perturbations, has been applied. The 16 nephron compliance tubule model with anti-phase oscillations produces stable regular pulse propagations.

4.4. Nephron Network Model for N = 72 Nephrons

Fig. 8 (a) shows the pressure variations in a rigid nephron network model with random initial states. The random initialization of the perturbations in the model shows that the pulses propagated toward the right and vanished. It has been observed that the model is stable with regular oscillations. Fig. 8 (b) shows the pressure variations in a rigid nephron network model with random initial states. The random initialization of the perturbations in the model

shows that the pulses propagated toward the right and vanished. It has been observed that the model is stable with regular oscillations. The impact of antiphase oscillations among the neighboring nephrons is very low.

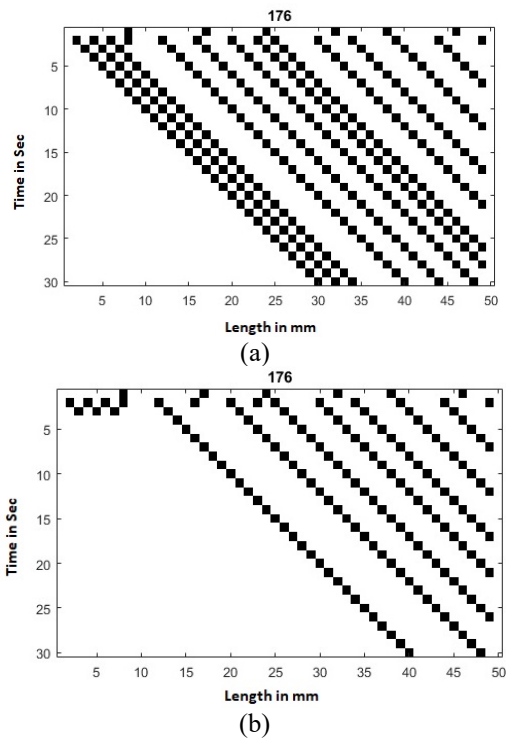


Fig. 7. Pressure variations in compliance nephron network model for CA rule 176 (a) with in-phase random initial states. (b) with out-of-phase random initial states

Fig. 9(a) shows the pressure variations in the compliance nephron network model with random initial states. Regular pulse propagation has been observed in the initial space length. However, the random initialization of the pulses produces irregular oscillations in the compliance 72 nephron model for further iterations. These irregular and unstable oscillations have become normal over a period of time. This pattern has been observed in the class III group of Wolfram CA rules. shows the pressure variations in the compliance nephron network model with random initial states. The regular pulse propagation has been observed in the initial space length. The random initialization of the pulses produces irregular oscillations in the compliance 72 nephron model for further iterations. These irregular and unstable oscillations have become normal over a period of time. This pattern has been observed in the class III group of Wolfram CA rules.

Fig. 9 (b) shows the pressure variations in the compliance nephron network model with random initial states. The regular pulse propagation has been observed in the initial space length. The random initialization of the pulses produces irregular oscillations in the compliance 72 nephron model for further iterations. These irregular and unstable oscillations have become normal over a period of

time. This pattern has been observed in the class III group of Wolfram CA rules.

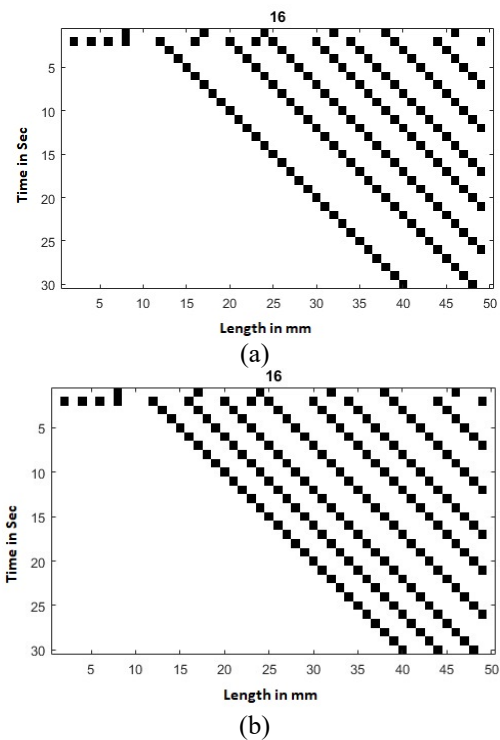


Fig. 8. Pressure variations in rigid nephron network model for CA rule 16 (a) with in-phase random initial states. (b) with out-of-phase random initial states

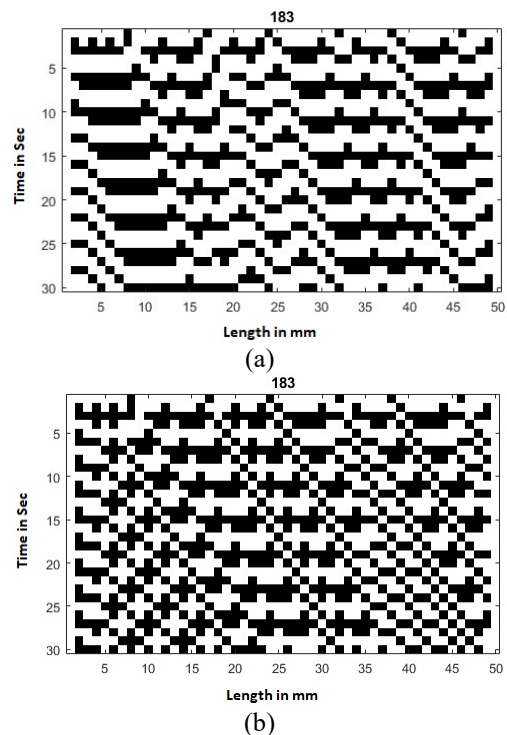


Fig. 9. Pressure variations in compliance nephron network model for CA rule 183 (a) with in-phase random initial states. (b) with out-of-phase random initial states

4.5. Nephron Network Model for N = 100 Nephrons

Fig. 10 (a) shows the pressure variations in a rigid nephron network model with the random initial state. The evolution pattern depicts irregular pulse propagation followed by regular pulse propagations. The irregular pulse propagation has been shifted towards the right. The in-phase oscillatory model for 100 nephrons depicts the unstable regular pulses.

Fig. 10 (b) shows the pressure variations in a rigid nephron network model with random initial states. The evolution pattern depicts irregular pulse propagation followed by regular pulse propagations. The irregular pulse propagation has been shifted towards the right. The anti-phase oscillatory model for 100 nephrons depicts the unstable pulses propagations.

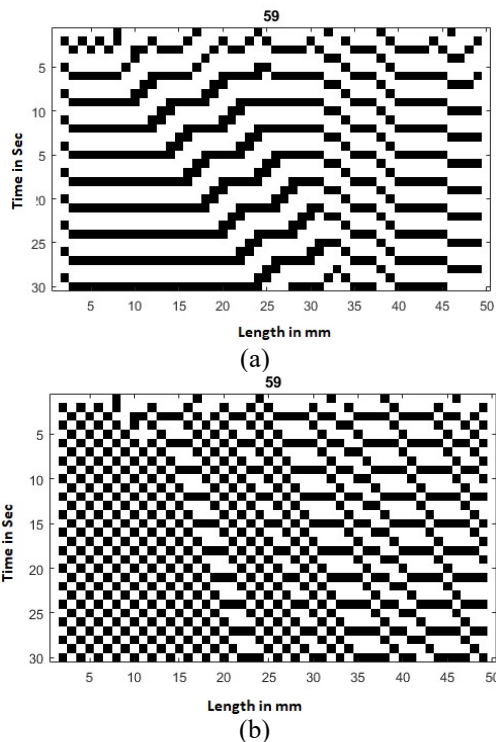


Fig. 10. Pressure variations in compliance nephron network model for CA rule 59 (a) with in-phase random initial states. (b) with out-of-phase random initial states

Fig. 11 (a) shows the pressure variations in the compliance nephron network model with random initial states. It exhibits pulse propagation towards the left. The irregular pulse propagation has been observed in the pattern evolution. The random initialization of the pulses produces irregular oscillations in the compliance 100 nephrons kidney model for further iterations. These irregular and unstable oscillations have become abnormal over a period of time. This pattern has been observed in the class III group of Wolfram CA rules.

Fig. 11 (b) shows the pressure variations in the compliance nephron network model with random initial

states. The pulse propagation observed within 100 nephrons compliance kidney model exhibits the performance of irregular pulse propagations. If the initialization of the pulse is in the middle, the pulse distorts the stable propagation and is constant for further iterations. It comes under class III property from Wolfram ECA rules. The evolution pattern over a period of time produces irregular oscillations. This model is unstable and produces irregular oscillations when it is distorted over further iterations.

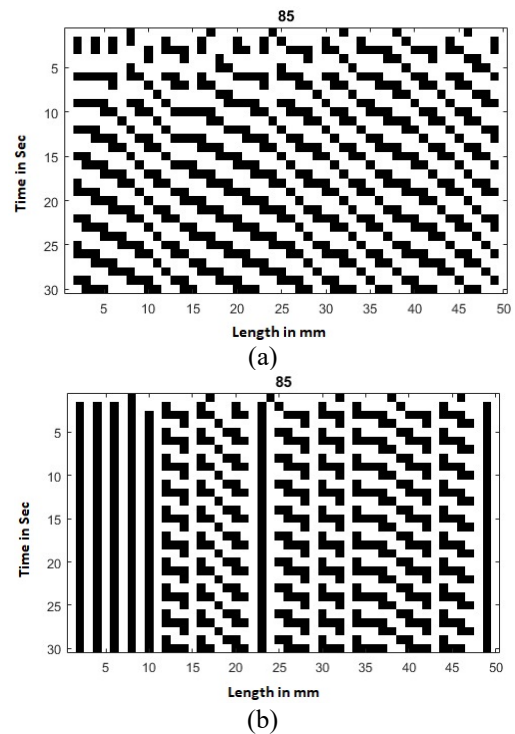


Fig. 11. Pressure variations in compliance nephron network model for CA rule 85 (a) with in-phase random initial states. (b) with out-of-phase random initial states

5. DISCUSSION

The oscillations observed in the multi-nephron network model are regular, periodic, and chaotic, which was also observed in the single nephron model in experimental analysis. In addition, the in-phase and out of synchronizations have been observed in the synchronization phenomena between interconnected nephrons. The emergent behavior that has been captured from the CA model is based on the necessary assumptions by adjusting the TGF gain in the nephron. The initialization of the current and previous states of the cells has achieved this adjustment of the TGF gain.

The pulses are continuous and above the threshold produced throughout the time evolution, causing the hypertensive pressure to have been observed in the out-of-phase oscillatory 8 and 10 nephrons, rigid network model. The normal stable period-doubling pulses propagated along the nephron network model have been observed in the in-

phase oscillatory 8 and 10 nephrons compliance network model. The unstable period-doubling pulses propagated along the nephron network model. These pulses are continuous pulses above the threshold. They are irregular and produced throughout evolution, causing hypertensive and chaotic pressure. It has been observed in the out-of-phase synchronization 8, 10, nephron compliance network model and in the in-phase 100 nephron compliance network model.

The normal stable period-doubling pulses propagated along the nephron network model produce a high pulse throughout the evolution when the perturbation is applied in the initial stages. These pulses are continuous above the threshold produced throughout evolution, causing hypertensive pressure. The pattern leads to irregular and complex behavior. It has been observed in the in-phase and anti-phase oscillatory 72 nephron compliance network model. It has been observed in the out-of-phase synchronization 100 nephrons, rigid network model.

Using the 8, 16 and 72 nephron models, we have established the model's validity, methods, and results compared to other multi-nephron simulations. These simpler models have also been helpful in developing an interpretation of the causes for behaviors that are expected to be seen in the simulation results from larger models. The eight-nephron system has been used to analyze the interaction between the competing coupling mechanisms of hemodynamic coupling and vascular signaling and investigate the stability of the pressure oscillations maintained by multiple loops of Henle in a kidney system. A 72-nephron system has been analyzed to increase the degree of vascular signaling in this system, resulting in higher-frequency pressure oscillations.

The emergent properties captured from the CA nephron network model clearly illustrate the behavior of the nephron that has been captured from the experimental analysis and numerical analysis. In-phase and out-of-phase synchronizations have been mainly observed from the CA model with various CA rules for the nephron network model under various TGF gains. Regular, periodic doubling and chaotic oscillations have been explicitly captured in the nephron network model along with the coupling behavior such as hemodynamic and vascular coupling. The evolution of the shock wave oscillations depicted in Fig. 3 (b) has been observed explicitly from the ECA rules in the nephron network model. The developed CA multi nephron model has been mimicking the functionality of the multi nephron from experimental findings under various pathological and physiological conditions.

6. CONCLUSION

The proposed CA framework for the nephron network model has demonstrated the study of emergent pressure flow using modular arithmetic and additive CA. The CA rules for multi-nephron network models for 8-nephron, 16-

nephron, 72-nephron and 100-nephron have been developed. The emergent properties of the CA multi-nephron network model have been compared with experimental analysis. By varying the TGF gains and the CA rules, we have observed the normotensive and hypertensive pressure-flow behavior with regular, periodic doubling, irregular oscillations, in-phase synchronization, and out-of-phase synchronization. The shock wave pulse propagation has been observed as global property from the evolutionary pattern. The multi-nephron network model developed with CA rules is able to capture the emergent dynamics of the kidney due to perturbations. The pressure dynamical behavior of a kidney is dependent on factors such as rigidity of the nephron tubule, interaction between nephrons, etc. As we increase the number of nephrons, the scope of the analysis is wider and offers numerous possibilities for different conditions of the kidney. The present paper has attempted to increase the number of nephrons, and has investigated the scalability problems that arise in the CA framework. This enables a path for simulating the whole kidney which has about one million nephrons.

REFERENCES

- Beard, D.A., Mescam, M. 2012. Mechanisms of pressure-diuresis and pressure-natriuresis in Dahl salt-resistant and Dahl salt-sensitive rats. *BMC Physiology*, 12, 1.
- Bohr, H., Jensen, K.S., Petersen, T., Rathjen, B., Mosekilde, E., Holstein-Rathlou, N.-H. 1989. Parallel computer simulation of nearest-neighbour interaction in a system of nephrons. *Parallel Computing*, 12, 113–120.
- Isojima, S., Grammaticos, B., Ramani, A., Satsuma, J. 2006. Ultradiscretization without positivity. *Journal of Physics A: Mathematical and General*, 39, 3663.
- Kanzaki, G., Tsuboi, N., Shimizu, A., Yokoo, T. 2020. Human nephron number, hypertension, and renal pathology. *The Anatomical Record*, 303, 2537–2543.
- Keener, J.P., Sneyd, J. 1998. *Mathematical physiology*, 1, Springer.
- Kesu, S.M.R., Ramasangu, H. 2021a. Spatio-temporal evolution of cellular automata based single nephron rigid tubular model. *The 12th International Conference on Computational Systems-Biology and Bioinformatics*, 90–97.
- Kesu, S.M.R., Ramasangu, H. 2021b. Cellular automata based coupled nephron model for pressure-driven oscillations, 2021 IEEE 18th India Council International Conference (INDICON), 1–6.
- Kesu, S.M.R., Ramasangu, H. 2022. Cellular automata model for emergent properties of pressure flow in single nephron compliance tubule. *Indonesian Journal of Electrical Engineering and Computer Science*, 25, 1227.
- Khouhak, J., Faghani, Z., Jafari, S. 2019. Wave propagation in a network of interacting nephrons. *Physica A: statistical mechanics and its applications*, 530, 121566.
- Khouhak, J., Faghani, Z., Laugesen, J.L., Jafari, S. 2020.

- The emergence of chimera states in a network of nephrons. *Chinese Journal of Physics*, 63, 402–409.
- Laugesen, J.L. 2011. Modelling nephron autoregulation and synchronization in coupled nephron systems. (Doctoral dissertation, Technical University of Denmark (DTU)).
- Layton, A.T. 2021. His and her mathematical models of physiological systems. *Mathematical Biosciences*, 108642.
- Layton, A. T., Edwards, A. 2014. *Mathematical Modeling in Renal Physiology*. Springer.
- Marsh, D.J., Postnov, D.D., Sosnovtseva, O., Holstein-Rathlou, N.-H. 2019. The nephron-arterial network and its interactions. *American Journal of Physiology-Renal Physiology*, 316, F769–F784.
- Marsh, D.J., Sosnovtseva, O., Mosekilde, E., Holstein-Rathlou, N.-H. 2007. Vascular coupling induces synchronization, quasiperiodicity, and chaos in a nephron tree. *Chaos: An Interdisciplinary Journal of Nonlinear Science*, 17, 15114.
- Marsh, D.J., Wexler, A.S., Brazhe, A., Postnov, D.E., Sosnovtseva, O., Holstein-Rathlou, N.-H. 2013. Multinephron dynamics on the renal vascular network. *American Journal of Physiology-Renal Physiology*, 304, F88–F102.
- Matsuya, K., Murata, M. 2013. Spatial pattern of discrete and ultradiscrete Gray-Scott model. ArXiv Preprint ArXiv:1305.5343.
- Moss, R. 2008. A clockwork kidney: Using hierarchical dynamical networks to model emergent dynamics in the kidney. Doctoral dissertation, University of Melbourne, Department of Computer Science and Software Engineering.
- Moss, R., Kazmierczak, E., Kirley, M., Harris, P. 2009. A computational model for emergent dynamics in the kidney. *Philosophical Transactions of the Royal Society A: Mathematical, Physical and Engineering Sciences*, 367, 2125–2140.
- Moss, R., Layton, A.T. 2014. Dominant factors that govern pressure natriuresis in diuresis and antidiuresis: A mathematical model. *American Journal of Physiology-Renal Physiology*, 306, F952–F969.
- Moss, R., Thomas, S.R. 2014. Hormonal regulation of salt and water excretion: A mathematical model of whole kidney function and pressure natriuresis. *American Journal of Physiology-Renal Physiology*, 306, F224–F248.
- Murata, M. 2013. Tropical discretization: Ultradiscrete Fisher–KPP equation and ultradiscrete Allen–Cahn equation. *Journal of Difference Equations and Applications*, 19, 1008–1021.
- Ohmori, S., Yamazaki, Y. 2015. Cellular automata for spatiotemporal pattern formation from reaction–diffusion partial differential equations. *Journal of the Physical Society of Japan*, 85, 14003.
- Ravasz, E., Barabási, A.-L. 2003. Hierarchical organization in complex networks. *Physical Review E*, 67, 26112.
- Ryu, H. 2014. Feedback-mediated dynamics in the kidney: Mathematical modeling and stochastic analysis (Doctoral dissertation, Duke University).
- Ryu, H., Layton, A.T. 2014. Tubular fluid flow and distal NaCl delivery mediated by tubuloglomerular feedback in the rat kidney. *Journal of Mathematical Biology*, 68, 1023–1049.
- Thomas, G. 2016. Simulation of whole mammalian kidneys using complex networks. Doctoral dissertation, University of Melbourne, Parkville, Victoria, Australia.
- Tokihito, T., Takahashi, D., Matsukidaira, J., Satsuma, J. 1996. From soliton equations to integrable cellular automata through a limiting procedure. *Physical Review Letters*, 76, 3247.
- Voorhees, B. 2012. Selfing dynamics in the rule space of additive cellular automata. *International Journal of General Systems*, 41, 609–616.
- Voorhees, B.H. 1996. Computational analysis of one-dimensional cellular automata, 15. World Scientific.
- Weisstein, E.W. 2002. Additive cellular automaton. <https://mathworld.wolfram.com/>.
- Ziganshin, A.R., Pavlov, A.N. 2005. Scaling properties of multimode dynamics in coupled chaotic oscillators. *Proceedings. 2005 International Conference Physics and Control*, 180–183. IEEE.